Check for updates

MISS LINHONG HE (Orcid ID : 0000-0002-7248-1259)

Article type : Research Article

Design, Synthesis and Biological Evaluation of Quinazoline Derivatives as Dual HDAC1 and HDAC6 Inhibitors for the Treatment of Cancer

Jinying Chen [b] †, Zitai Sang [c] †, Youjun Jiang [b], Chao Yang [b], Linhong He [a,#]

[a] Pharmaceutical College, Guangxi Medical University, Nanning, Guangxi, China.

[b] SinoGrain Chengdu Storage Research Institute Co.Ltd

[c] State Key Laboratory of Biotherapy, West China Hospital, West China Medical School, Sichuan University, Chengdu, Sichuan, PR China.

Running Title: Dual HDAC1 and HDAC6 inhibitors for the treatment of cancers

Correspondence

Linhong He, Pharmaceutical College, Guangxi Medical University, Nanning, Guangxi, China. E-mail: HLhongedu@163.com.

This article has been accepted for publication and undergone full peer review but has not been through the copyediting, typesetting, pagination and proofreading process, which may lead to differences between this version and the Version of Record. Please cite this article as doi: 10.1111/cbdd.13405

This article is protected by copyright. All rights reserved.

Accepted Article

Accepted Article

Keywords: dual inhibitors, HDAC, SAR study, cancer

Abstract

Fifty-eight quinazoline based compounds were designed and synthesized based on the structural optimizations from the lead compound **23bb** in an attempt to search for more potent dual HDAC1 and HDAC6 inhibitors. Among them, **32c** (HDAC1, IC_{50} = 31.10 ± 0.37 nM; HDAC6, IC_{50} = 16.15 ± 0.62 nM) and **32d** (HDAC1, IC_{50} = 37.00 ± 0.24 nM; HDAC6, IC_{50} = 35.00 ± 0.71 nM) were not only identified as potent dual-acting HDAC1 and HDAC6 inhibitors with over 10-fold selectivity to the other HDACs, but also displayed activities in tubulin acetylation and histone H_3 acetylation induction. Importantly, both of them displayed strong antiproliferative activities against various tumor cell lines *in vitro* with IC_{50} values less than 40 nM, especially for hematological tumors cells (U266 and RPMI8226, IC_{50} < 1 nM), which were even better than **23bb** and SAHA. Furthermore, **32c** showed a significant tumor growth inhibition (antitumor rate = 63.98%, p<0.05) in the resistant MCF-7/ADR xenograft model without any obvious body weight changes and abnormal behaviors. Our findings validate that **32c** is a potent dual inhibitor of HDAC1/6 that can be an efficacious treatment for breast cancer with adriamycin resistance.

Introduction

Histone deacetylases (HDACs) have been identified as attractive targets for cancer therapeutics, which are responsible for deacetylation of lysine resides in histone and non-histone substrates (p53 and tubulin), and play important roles in regulating various tumor suppressor pathways (1-5). Until now, 18 human HDACs have been categorized into four classes: class I (HDAC1, 2, 3 and 8), class II (class IIa: HDAC4, 5, 7 and 9; class IIb: HDAC6 and 10), class III (sirtuins, SIRT1-7) and class IV (HDAC11) (3). All the HDACs are zinc-dependent enzymes with a highly

This article is protected by copyright. All rights reserved.

Accepted Article

conserved catalytic site except class III that requires NAD^+ as a cofactor (3,6). Although the biological functions of many HDACs subtypes are still being defined, there are compelling evidences that class I HDACs and HDAC6 overexpress in a variety of cancers, including colorectal cancer, prostate cancer, breast cancer, hepatocellular carcinoma (3,7,8). Besides, more and more HDAC inhibitors (**Figure 1**) have been proven to induce growth arrest, differentiation, and apoptosis in cancer cells, as well as suppress *in vivo* tumor growth (3, 6). Therefore, HDAC inhibitors are emerging as a new class of chemo-therapeutic agents.

Figure 1

Up to now, four HDAC inhibitors (Vorinostat, Romidepsin, Belinostat and Panobinostat) approved by the US FDA have been proven to inhibit either all or at least several HDAC members, which may trigger numerous side effects and low potencies (6, 13). Meanwhile, single target drugs could not meet the clinical demand due to their various drug resistance phenomena (9-10). To achieve curative effects against tumors with fewer side effects, continuous efforts in this field has been focused on the development of dual-acting (HDAC–Topo I) or triple (HDAC 1-3) inhibitors (9-11). Since Dual-acting HDAC1 and HDAC6 inhibitors not only can potently inhibit tumor growth, but also protect cortical neurons against hypoxia-induced toxicity (3,7,8), developing dual inhibitors targeting HDAC1 and HDAC6 is a promising and attractive strategy to broad their application in the treatment of cancers, especially for solid tumors (8,11,12).

HDAC inhibitors generally consist of three canonical pharmacophoric characteristics, a zinc binding group (ZBG) that chelates the active site Zn^{2+} ion, a surface recognition cap group that interacts with the amino acid residues presenting at the surface of the HDAC, and a linker unit between the former two parts (3). Numerous investigations claimed that a hydroxamic acid group is the most common ZBG forming one or more hydrogen bonds with histone deacetylase homologue

This article is protected by copyright. All rights reserved.

Accepted Article

(**Figure 1**) (3,6). In our previous study, we have deeply investigated the structure activity relationship (SAR) of the cap group that may contribute an important function to the selective activity. A series of fragments were respectively docked into HDAC1 (PDB code 4BKX) and HDAC6 (homology model) (3). Among them, 2-methylquinazoline was picked out since it can comfortably occupy the surface groove and form robust interaction with HDACs (3). Additionally, it indeed displayed excellent inhibitory activity against HDAC1 and HDAC6 (3). Based on the initial leading compound 23bb (HDAC1, IC_{50} = 422 nM; HDAC6 IC_{50} = 17 nM) with favorable anti-tumor activity, we plan to get insights into its SAR and rationally modify its cap and linker regions to seeking new dual HDAC1 and HDAC6 inhibitors. In this paper, we report the synthesis and pharmacological evaluation of fifty-eight compounds with antitumor activities, as well as inhibitory activities against HDAC1 and HDAC6, of which the promising compounds **32c** and **32d** were further conducted in resistant MCF-7/ADR xenograft model *in vivo* to find the optimal candidate compound.

Figure 2

1. Chemistry

A common route was applied for the synthesis of compounds **6a-6jj** (**Scheme 1**). Commercially available material, 2-methoxy-5-nitrophenol (**1**), was treated with ethyl 4-bromobutanoate in an alkaline condition to afford intermediate **2**, which was reduced to aniline derivative **3** with hydrogen and Palladium/C. Then **3** was reacted with 4-chloro-2-methylquinazoline at room temperature (rt) to provide **4** in a good yield. A variety of halogenated reagents were respectively introduced to **4** via microwave heating to prepare **5a-5jj**, which could improve the reaction speed and yield. Target hydroxamic acid compounds **6a-6jj** were directly converted through reacting **5a-5jj** with hydroxylamine.

This article is protected by copyright. All rights reserved.

Accepted Article

Scheme 1

To study the SAR of linker with different length alkyl chains, novel compounds **14a-14f** were prepared according to **Scheme 2**. The phenolic hydroxyl group (**7**) was firstly protected by chloromethyl methyl ether (MOMCl) to give **8**, which was reduced with hydrogen and coupled with 4-chloro-2-methylquinazoline in sequence to give intermediate **10**. The further N-methylated for **10** was carried out in a strong alkaline condition with iodomethane to offer **11**, whose protection group was removed using saturated hydrogen chloride in ethyl acetate, giving the key intermediate **12**. The subsequent reactions were the same as **Scheme1**.

Scheme 2

Another kind of linker, different amide alkyl chains, was also explored to search more potent HDAC inhibitors. Final compounds **20a-20e** were prepared according to **Scheme 3**, and the reaction procedures were the same as **Scheme 1**.

Scheme 3

Next, we also focused on the linker position on phenyl group. As shown in **Scheme 4**, N-methyl-4-nitroaniline (**21**) and 4-chloro-2-methylquinazoline were used as the starting materials, and the following reactions were similar as in **Scheme 1**. Eventually, target compounds **25a-25e** were obtained.

Scheme 4

Based on the SAR analysis of those new compounds, **32a-32f** were also synthesized according to **Scheme 5**. 4-Fluoro-3-nitroaniline (**26**) was reacted with sodium methoxide to give **27**, which was treated with corresponding reactants in the same procedures mentioned above to offer the resulting compounds **32a-32f**.

Scheme 5

This article is protected by copyright. All rights reserved.

Accepted Article

2. Result and discussion

2.1 Antiproliferative activity tests for synthesized compounds

Given that the lead compound **23bb** could significantly inhibit HCT116 cells to proliferation (3), all synthesized derivatives were conducted to assess their antiproliferative activities against HCT116 cells using MTT assay. The primary tested concentrations for compounds were set as 5 μM, 500 nM, 50 nM and 5 nM to find out candidate compounds as many as possible. As summarized in **Table 1**, **23bb** with a methyl on R_1 position displayed a good potency. Compounds replacing the methyl by a substituted group containing branched chains or distinct benzyl group, such as **6c-g**, **6k-o**, **6aa-6jj**, completely lost their activities, which may result from steric hindrance effect and long side chains contributed to steric effects in a certain degree. Interestingly, **6j** was more potent than **6a**, despite the fact that the volume of allyl group is larger than ethyl. Similar trend was observed between **6h** and **6g**, which may be attributed to their good conjugation. When linked with electron-donor and electron-acceptor, the charge transfer is obvious, thus showed a good potency. Taking into account the SAR known from **23bb**'s discovery program and our first modifications on R_1 position, it was very likely that N-substituted-N,2-dimethylquinazoline fragment was the optimal cap.

Table 1

Results from the comparisons of **23bb** and **14b**, or **20c** and **25c**, demonstrated that compounds moving the linker from 3'-phenyl to 4'-phenyl led to different degrees of loss in activities. Moreover, compounds upon introducing a methoxy at 4'-phenyl (**23bb**, **32c** and **32d**) significantly increased potencies, whose IC_{50} values were less than 50 nM, indicating that this methoxy was necessary to improve activity. Variation of the linker length verified the optimal distance between phenyl and hydroxamic acid was 4-atom, while 5-atom slightly reduced the potency, see compounds **20c** and **20d**, or **32c** and **32d**. Instead of ether chain at 3'-phenyl, the

This article is protected by copyright. All rights reserved.

amide hydrocarbon chain owned better activity by comparison **23bb** and **32c**. In brief, the importance of the changes on **23bb**'s cap and linker regions was summarized in **Figure 3**.

Figure 3

2.2 Inhibitory activities against HDAC1 and HDAC6

In an attempt to confirm their potential inhibitory activities against HDAC1 and HDAC6 isoforms, compounds (**6a**, **6h**, **6j**, **14a**, **14f**, **20c**, **32a**, **32b**, **32c** and **32d**) potently inhibiting HCT116 cells to growth were further evaluated. Interestingly, the inhibitory activities against HDAC6 not HDAC1 for all tested compounds were in line with the SAR mentioned above (**Table 2**). However, apart from **14f**, all the compounds increased the potencies of inhibiting HDAC1 in contrast to **23bb**. Although slight potencies decrease versus the positive control SAHA, both **32c** and **32d** significantly inhibited the activities of HDAC1 and HDAC6, whose inhibitory activities against HDAC1 were much better than that of **23bb**. To highlight the inhibition of **32c** and **32d** towards HDAC1 and HDAC6, automated docking studies were carried out using the Discovery studio 2.1 software. As expected, **32c** and **32d** matched perfectly with the configuration of the binding sites of HDAC1 and HDAC6, whose results were consist with their enzyme potencies (Supplementary Material **Figure S1**).

Table 2

2.3 Antiproliferative activity tests for selected compounds

Since HDAC1 and HDAC6 have been verified to play important roles in various types of cancers, whose inhibitors have demonstrated potencies as novel therapeutics in preclinical and clinical studies of both solid and haematological cancers, compounds **32a-32d** were selected to investigate their antiproliferative activities against another eight tumor cell lines on the basis of their satisfied potencies *in vitro*, including solid tumors (liver cancer HepG2 cells, breast cancer M-M-231and MCF-7

This article is protected by copyright. All rights reserved.

Accepted Article

Accepted Article

cells, lung cancer H1975 and H460 cells, and cervical cancer Hela cells) and hematological tumors (myeloma U266 and RPMI8226 cells). As listed in **Table 3**, all of them could significantly suppress the proliferation for tested cell lines (IC_{50} < 400 nM). As expected, myeloma U266 and RPMI8226 cells were presented the best inhibition, in accordance with the fact that most of the current HDAC inhibitors were used for the treatment of hematologic malignancies, but a lack of visible efficacy against solid tumors (3). Among them, **32c** and **32d** showed significant antipoliferative potentials with IC_{50} values ranging from 0.01 to 40 nM in these tumor cell lines, which were much better than **23bb** and SAHA. It turned out that both **32c** and **32d** could not only be used in the therapy of hematologic malignancies, but also solid tumors.

Table 3

2.4 HDAC isoform selectivity for 32c and 32d

Since both **32c** and **32d** exhibited potent bioactivities *in vitro*, they were further determined for the activities on the other HDAC isoforms. As summarized in **Table 4**, compound **32c** was potent at 1000 nM against class one HDACs and HDAC6, but at more than one micromolar level against the other HDACs. Similar trend was observed by **32d**. What's more, both of them showed over 10-fold selectivity of HDAC1 or HDAC6 relative to the inhibition of HDAC2, HDAC3 and HDAC8, indicating that **32c** and **32d** were dual-acting HDAC1 and HDAC6 inhibitors.

Table 4

2.5 Tubulin acetylation and H_3 acetylation test

Cytoblot experiments were performed to evaluate the histone H_3 (a known substrate for HDACs 1, 2 and 3) acetylation (Ac-H_3) and tubulin (a known substrate for HDAC6) acetylation (Ac-Tub) for compounds **32c** and **32d** in Hela cells. As expected, both of them displayed better Ac-Tub activities than Ac-H_3 (**Table 5**), which were in consistent with the *in vitro* enzymatic data, indirectly demonstrating

This article is protected by copyright. All rights reserved.

Accepted Article

that **32c** and **32d** owned a slightly better inhibition to HDAC6 than HDAC1. Additionally, **32c** showed better activity than **23bb** and SAHA in both situations.

Table 5

2.6 Immunofluorescence staining

Since recent reports have highlighted HDAC involvement in the deacetylation of not only histone regulatory proteins, but also important non-histone ones, such as tubulin (2, 3, 9), compounds **32c** and **32d** were further investigated their potencies of inhibiting tubulin polymerization or de-polymerization by immunofluorescence staining. Paclitaxel (PTX) was selected as microtubules polymerizer and MPC6827 was an anti-tubulin agent. As shown in **Figure 4**, the morphology of microtubules and spindles in H460 cells treated with **32c** and **32d** for 12 h were significantly suppressed the microtubule polymerization and spindle formation, which were similar to those incubated with MPC6827, but not PTX, demonstrating that **32c** and **32d** possessed the potencies of preventing tubulins to form microtubules. Those results confirmed that the favorable anti-tumor activities of these dual-acting HDAC1 and HDAC6 inhibitors may be attributed from the inhibition of tubulins to form microtubules.

Figure 4

2.7 Anti-tumor activity in MCF-7 xenograft model

To determine the anti-tumor potencies of compounds **32c** and **32d** in drug resistant tumor xenograft model *in vivo*, human breast cancer MCF-7/ADR model were established, and a broad spectrum anticancer drug Adriamycin (ADM) was set as positive control. 30 Balb/C mice were randomly assigned to four groups when the tumor volumes reached about a size of 100 mm^3. Treatment groups respectively received tail intravenously ADM (4 mg/kg, every 7 days), **32c** (2.5 kg/kg, every 2 days) and **32d** (5 mg/kg, every 2 days) for 34 days, and the vehicle (control) group mice were given equal amount of physiological saline every 2 days in the same way.

This article is protected by copyright. All rights reserved.

Accepted Article

As shown in Figure **5B-D**, **32c** caused a remarkable reduction in tumor growth (63.98%, $p<0.05$) as compared with administration of vehicle only, which was better than **32d** (48.72%, $p<0.05$) and the positive control ADM (16.1%). As expected, the tumor growth inhibition of reference drug ADM was low since it had developed resistance to MCF-7/ADM cell line. Moreover, ADM-treated mice were observed obvious loss of body weight. However, the optimal compound **32c** treatment group exhibited no significant body weight changes and abnormal behaviors, which were a little better than that of **32d**-treated mice. These results proved that **32c** was an effective compound for the treatment of ADM resistant breast cancer without significant toxicity.

Figure 5

3. Conclusion

Fifty-eight quinazoline based compounds were synthesized, and their bioactivities *in vitro* revealed a relatively clear SAR. Compounds **32a-d** displayed strong antiproliferative activities against various tumor cell lines, including solid tumors (HCT116, HepG2, M-M-231, MCF-7, H460, H1975, H460 and Hela cells) and hematological tumors (U266 and RPMI8226 cells). Among them, **32c** and **32d** were not only identified as good dual-acting HDAC1 and HDAC6 inhibitors with over 10-fold selectivity to the other isoforms, but also exhibited good activities in tubulin acetylation and histone H_3 acetylation induction, of which **32c** was even better than **23bb** and SAHA. Additionally, both of them could effectively suppress tubulins to form microtubule that was supposed to potently enhance their anti-tumor activities. In the resistant MCF-7/ADR xenograft animal model, **32c** significantly inhibited tumor growth without significant weight changes and abnormal behaviors, which was better than **32d**. Hence, further investigation of compound **32c** is ongoing and will be reported in due time.

This article is protected by copyright. All rights reserved.

Accepted Article

Acknowledgments

We are grateful to the National Key Programs of China during the 13th Five-Year Plan Period.

Conflict of Interest

The authors have declared no conflict of interest.

Supplementary Material

Docking studies: **32c** and **32d** were docked into HDAC1 and HDAC6, respectively.

Experimental section: Synthetic details, characterization data for all compounds, and biological procedure reported in this manuscript.

NMR Spectrum: ^{1}H- and ^{13}C-NMR spectrum of all final new compounds.

References and notes

1. Minucci S., Pelicci P.G. (2006) Histone deacetylase inhibitors and the promise of epigenetic (and more) treatments for cancer. *Nat. Rev.Cancer*. 6: 38-51.

2. Hubbert C., Guardiola A., Shao R., Kawaguchi Y., Ito A., Nixon A., Yoshida M., Wang X. F., Yao T.P. (2002) HDAC6 Is a Microtubule-Associated Deacetylase. *Nature*. 417: 455-458.

3. Yang Z., Wang T., Wang F., Niu T., Liu Z., Chen X., Long C., Tang M., Cao D., Wang X., Xiang W., Yi Y., Ma L., You J., Chen L. (2016) Discovery of Selective

This article is protected by copyright. All rights reserved.

Accepted Article

Histone Deacetylase 6 Inhibitors Using the Quinazoline as the Cap for the Treatment of Cancer. *J. Med. Chem*. 59:1455-1470.

4. Zhou Y., Dun Y., Fu H., Wang L., Pan X., Yang X., Fang H. (2017) Design, synthesis, and preliminary bioactivity evaluation of N-benzylpyrimidin-2-amine derivatives as novel histone deacetylase inhibitor. *Chem. Biol. Drug Des*. 90: 936-942.

5. Zhang S., Huang W., Li X., Yang Z., Feng B. (2015) Synthesis, Biological Evaluation, and Computer-Aided Drug Designing of New Derivatives of Hyperactive Suberoylanilide Hydroxamic Acid Histone Deacetylase Inhibitors. *Chem. Biol. Drug Des*. 86: 795-804.

6. Cheng J., Qin J., Guo S., Qiu H., Zhong Y. (2014) Design, synthesis and evaluation of novel HDAC inhibitors as potential antitumor agents. *Bioorg. Med. Chem. Lett*. 24: 4768-4772.

7. Sun Q., Yao Y., Liu C., Li H., Yao H., Xue X., Liu J., Tu Z., Jiang S. (2013) Design, synthesis, and biological evaluation of novel histone deacetylase 1 inhibitors through click chemistry. *Bioorg. Med. Chem. Lett*. 23: 3295-3299.

8. Tsai H., Wu J., Kao M., Chen J., Sun G.Y., Ong W., Lin T. (2016) *Clinacanthus nutans* Protects Cortical Neurons Against Hypoxia-Induced Toxicity by Downregulating HDAC1/6. *NeuroMol*. Med. 18: 274.

9. Guerrant W., Patil V., Canzoneri J.C., Yao L., Hood R., Oyelere D.K. (2013) Dual-acting histone deacetylase-topoisomerase I inhibitors. *Bioorg. Med. Chem. Lett*. 23: 3283-3287.

10. Jadhavar P.S., Ramachandran S.A., Riquelme E., Gupta A., Quinn K.P., Shivakumar D., Ray S., Zende D., Nayak A.K., Miglani S.K., Sathe B.D., Raja M., Farias O., Alfaro I., Belmar S., Guerrero J., Bernales S., Chakravarty S., Hung D.T., Lindquist J.N., Rai R. (2016) Targeting prostate cancer with

This article is protected by copyright. All rights reserved.

Accepted Article

compounds possessing dual activity as androgen receptor antagonists and HDAC6 inhibitors. *Bioorg. Med. Chem. Lett*. 26: 5222-5228.

11. Ma X., Lv X., Zhang J. (2018) Exploiting polypharmacology for improving therapeutic outcome of kinase inhibitors (KIs): An update of recent medicinal chemistry efforts. *Euro. J. Med. Chem*. 143: 449-463.

12. Wen J., Niu Q., Liu J., Bao Y., Yang J., Luan S., Fan Y., Liu D., Zhao L. (2016) Novel thiol-based histone deacetylase inhibitors bearing 3-phenyl-1*H*-pyrazole-5-carboxamide scaffold as surface recognition motif: Design, synthesis and SAR study. *Bioorg. Med. Chem. Lett*. 26: 375-379.

13. Zhang Q., Lu B., Li J. (2017) Design, synthesis and biological evaluation of 4-piperazinyl-containing Chidamide derivatives as HDACs inhibitors. *Bioorg. Med. Chem. Lett*. 27: 3162-3166.

Caption

Figure 1. Examples of HDAC inhibitors.

Figure 2. The idea to explore the SAR of compound **23bb**.

Figure 3. Graphical representation of SAR for quinazoline based compounds with antiproliferative activities against HCT116.

Figure 4. Effect of compounds **PTX**, **MPC6828**, **32c** and **32d** on the microtubule in H460 cells. Treated cells were respectively incubated with compounds **PTX**, **MPC6828**, **32c** and **32d** at concentrations of 1 nM and 10 nM for 12 h, then the untreated (control) and treated cells were fixed in methanol and stained with α-tubulin and counterstained with 4,6-diamidino-2-phenylindole (DAPI). Microtubules and unassembled tubulin are shown in green. DNA, stained with DAPI, is shown in blue.

This article is protected by copyright. All rights reserved.

Accepted Article

Figure 5. Anti-tumor activities of **32c**, **32d** and ADM on the MCF-7ADR xenograft models. Body weight (A) and tumor volume (B) of mice were measured every other day during the treatment. Solid tumors were got by sacrificing those mice after 34 days' treatment, then measured (C) and photographed (D). *$p < 0.05$, significantly different compared with control.

Scheme 1. Synthesis of **6a-6jj**. Reagents and conditions: (**a**) $Br(CH_2)_3COOEt$, Cs_2CO_3, MeCN, reflux; (**b**) H_2, Pd/C (5%), MeOH, rt; (**c**) 4-Chloro-2-methylquinazoline, Me_2CHOH, rt; (**d**) $R_1Cl(R_1Br)$, K_2CO_3, KI, DMF, MW (80 W,100 ºC, 1 h) . (**e**) 50% NH_2OH (aq), NaOH, DCM/MeOH (v/v, 1/2), rt.

Scheme 2. Synthesis of **14a -14f**. Reagents and conditions：(**a**) NaH, MOMCl, DMF, 0 °C to rt; (**b**) H_2, Pd/C (5%), MeOH, rt; (**c**) 4-Chloro-2-methylquinazoline, Me_2CHOH, rt; (**d**) NaH, CH_3I, DMF, 0 °C to rt; (**e**) EtOAc, HCl; (**f**) $Br(CH_2)_nCOOEt$, Cs_2CO_3, MeCN; (**g**) 50% NH_2OH (aq), NaOH, DCM/MeOH (v/v, 1/2), rt.

Scheme 3. Synthesis of **20a-20e**. Reagents and conditions：(**a**) 4-Chloro-2-methylquinazoline, Me_2CHOH, rt; (**b**) NaH, CH_3I, DMF, 0 °C to rt; (**c**) H_2, Pd/C (5%), MeOH, rt; (d) $ClCO(CH_2)_nCOOEt$, Et_3N, DCM, rt; (**e**) 50% NH_2OH (aq), NaOH (K_2CO_3), DCM/MeOH (v/v, 1/2), rt.

Scheme 4. Synthesis of **25a-25e**. Reagents and conditions: (**a**) 4-Chloro-2-methylquinazoline, Me_2CHOH, rt; (b) H_2, Pd/C (5%), MeOH, rt; (**c**) $ClCO(CH_2)_nCOOEt$, Et_3N, DCM, rt; (**d**) 50% NH_2OH (aq), NaOH (K_2CO_3), DCM/MeOH (v/v, 1/2), rt.

Scheme 5. Synthesis of **32a-32f**. Reagents and conditions: (**a**) CH_3ONa, MeOH, rt; (**b**) 4-Chloro-2-methylquinazoline, Me_2CHOH, rt; (**c**) NaH, CH_3I, DMF, 0 °C to rt; (**d**) H_2, Pd/C (5%), MeOH, rt; (**e**) $ClCO(CH_2)_nCOOEt$, Et_3N, DCM, rt; (**f**) 50% NH_2OH (aq), NaOH (K_2CO_3), DCM/MeOH (v/v, 1/2), rt.

This article is protected by copyright. All rights reserved.

Table 1. Antiproliferative activities of all the synthesized compounds against HCT116 cells [a]

Comp.	potency	Comp.	potency	Comp.	potency	Comp.	potency
6a	++	**6p**	+	**6ee**	-	**20d**	+
6b	+	**6q**	+	**6ff**	-	**20e**	+
6c	-	**6r**	-	**6gg**	-	**25a**	++
6d	-	**6s**	-	**6hh**	-	**25b**	+
6e	-	**6t**	+	**6ii**	-	**25c**	+
6f	-	**6u**	-	**6jj**	-	**25d**	+
6g	-	**6v**	+	**14a**	++	**25e**	-
6h	++	**6w**	-	**14b**	+	**32a**	++
6i	-	**6x**	+	**14c**	+	**32b**	++
6j	++	**6y**	+	**14d**	+	**32c**	++++
6k	-	**6z**	+	**14e**	-	**32d**	+++
6l	-	**6aa**	-	**14f**	++	**32e**	+
6m	-	**6bb**	-	**20a**	+	**32f**	+
6n	-	**6cc**	-	**20b**	+	**23bb**	+++
6o	-	**6dd**	-	**20c**	++		

[a] The test of antiproliferative activities against HCT116 cells for all synthesized compounds were conducted with four concentrations: 5 μM, 500 nM, 50 nM and 5 nM. Thus, "-" means inhibition rate less than 50% at 5 μM, "+" means inhibition rate over 50% at 5 μM, "++" means inhibition rate over 50% at 500 nM, "+++" means inhibition rate over 50% at 50 nM, "++++" means inhibition rate over 50% at 5 nM. Data are expressed as the mean ± SD from at least three independent experiments.

Accepted Article

This article is protected by copyright. All rights reserved.

Table 2. The inhibitory activities of selected compounds against HDAC1 and HDAC6 [a]

Comp.	IC_{50} (nM)		Comp.	IC_{50} (nM)	
	HDAC1	**HDAC6**		**HDAC1**	**HDAC6**
6a	272.10±3.44	76.23±0.71	**20c**	395.23±3.01	82.04±1.23
6h	591.40±2.99	120.30±1.00	**32a**	108.20±1.33	59.27±2.08
6j	364.60±4.70	45.28±1.29	**32b**	87.46±1.03	50.16±1.00
14a	31.06±0.83	85.37±2.00	**32c**	31.10±0.37	16.15±0.62
14f	578.26±1.96	322.94±2.02	**32d**	37.00±0.24	35.00±0.71
23bb	422.00±0.93	19.03±1.80	**SAHA**	11.40±0.39	16.01±1.37

[a] Compounds were tested in the 8-dose IC_{50} mode in duplicate with 5-fold serial dilutions starting at 5 μM. The IC_{50} values are the mean of at least two experiments.

Accepted Article

This article is protected by copyright. All rights reserved.

Accepted Article

Table 3. Activities of compounds **32a-32d** and **23bb** against various tumor cell Lines [a]

Comp.	IC_{50} (nM)							
	HepG2	**M-M-231**	**MCF-7**	**H1975**	**H460**	**Hela**	**U266**	**RPMI8226**
32a	46.73±1.20	38.51±1.52	40.94±2.07	121.03±1.06	376.34±19.20	59.28±0.49	1.06±0.37	2.91±0.61
32b	4.77±0.72	14.29±1.03	12.51±0.92	31.71±0.77	230.63±2.80	13.86±1.23	1.54±0.04	2.98±0.30
32c	3.50±0.48	2.65±0.71	2.55±0.40	2.88±0.69	1.05±0.02	2.41±0.59	＜0.01	＜0.01
32d	4.51±0.33	7.41±0.81	8.62±1.01	39.51±1.00	37.59±2.62	3.16±0.15	0.15±0.01	0.37±0.21
23bb	39.07±1.11	-	-	-	55.13±4.72	50.02±0.74	13.83±1.01	52.21±0.66
SAHA	>1000	>1000	>1000	>1000	>1000	720±13.02	569±21.00	420±9.37

[a] IC_{50} = compound concentration required to inhibit tumor cell proliferation by 50%. Data are expressed as the mean ± SD from the dose-response curves of at least three

independent experiments.

This article is protected by copyright. All rights reserved.

Table 4. HDAC inhibition activities of compounds **32c** and **32d** [a]

isoform	IC_{50} / nM			
	32c	**32d**	**23bb**	**SAHA**
HDAC1	31.10±0.37	37.00±0.24	422.00±0.93	11.40±0.39
HDAC2	349±12.05	512.08±21.49	390.01±5.41	34.98±3.06
HDAC3	401±18.99	510.66±9.43	410.29±10.21	32.10±2.77
HDAC8	934.17±42.01	>1000	>1000	170.00±19.02
HDAC4	>1000	>1000	>1000	>1000
HDAC5	>1000	>1000	>1000	>1000
HDAC7	>1000	>1000	>1000	>1000
HDAC9	>1000	>1000	>1000	>1000
HDAC6	16.15±0.62	35.00±0.71	19.03±1.80	16.01±1.37
HDAC10	>1000	>1000	>1000	170.00±15.32
HDAC11	>1000	>1000	>1000	>1000

[a] Compounds were tested in the 8-dose IC_{50} mode in duplicate with 5-fold serial dilutions starting at 10 μM. The IC_{50} values are the mean of at least two experiments.

Accepted Article

This article is protected by copyright. All rights reserved.

Table 5. H_3 acetylation and tubulin acetylation induction in Hela cell of compounds **32c** and **32d** [a]

	EC_{50}/nM			
	32c	**32d**	**23bb**	**SAHA**
Ac-H_3	170±9.22	217.20±11.93	1739.03±83.91	377.02±9.03
Ac-Tub	43.92±6.07	75.33±6.00	59.00±10.28	401.11±13.97

[a] EC_{50} values of tubulin acetylation and Ac-H_3 are based on ELISA experiments run in duplicate in Hela cell. Data are expressed as the mean ± SD from the dose-response curves of at least three independent experiments.

Accepted Article

This article is protected by copyright. All rights reserved.

Accepted Article

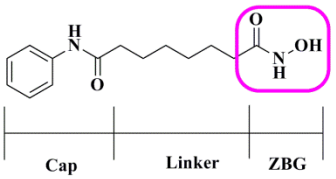

Vorinostat (SAHA)

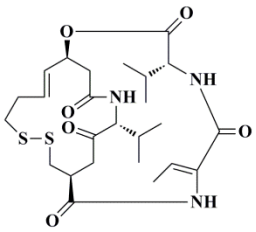

Romidepsin

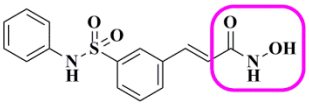

Belinostat

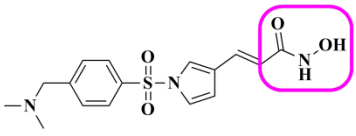

Resminostat

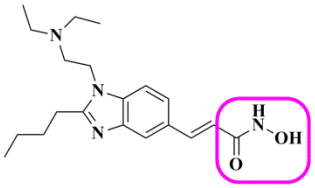

Pracinostat

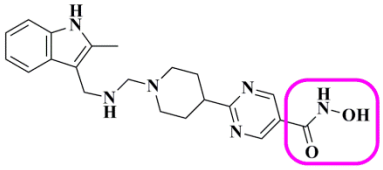

Quisinostat

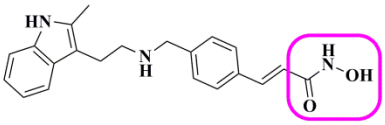

Panobinostat

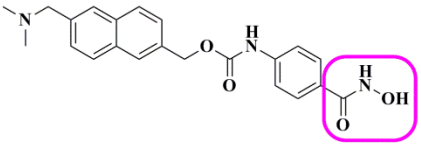

Givinostat

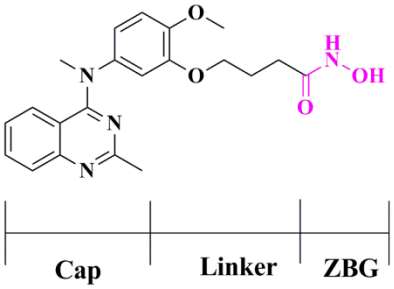

23bb

SAR exploring

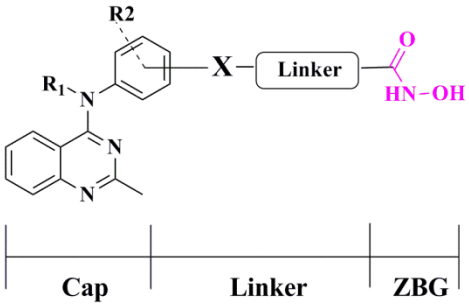

This article is protected by copyright. All rights reserved.

Accepted Article

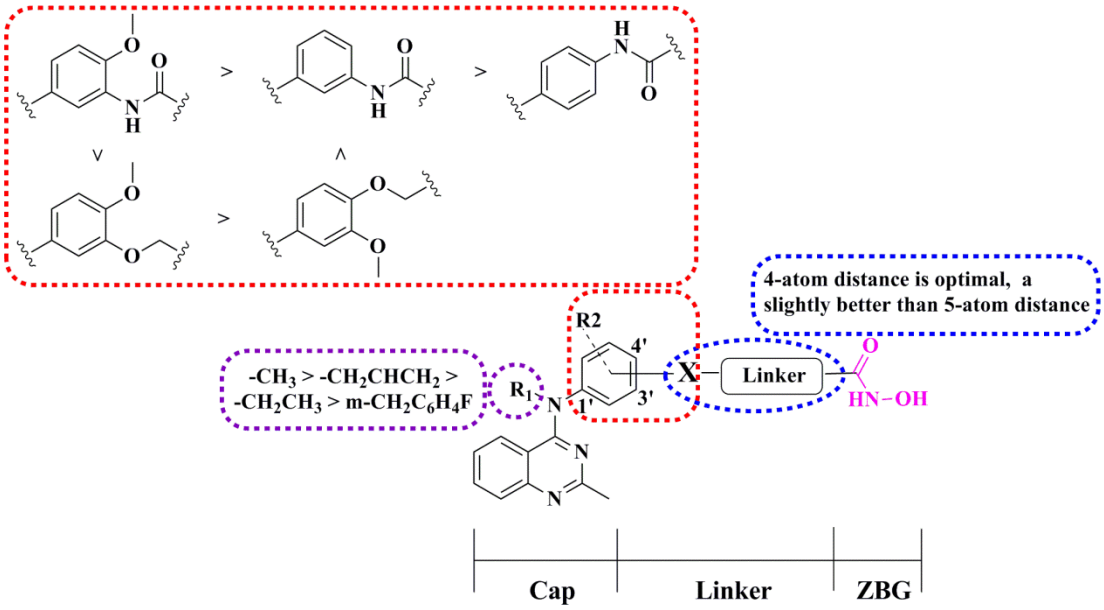

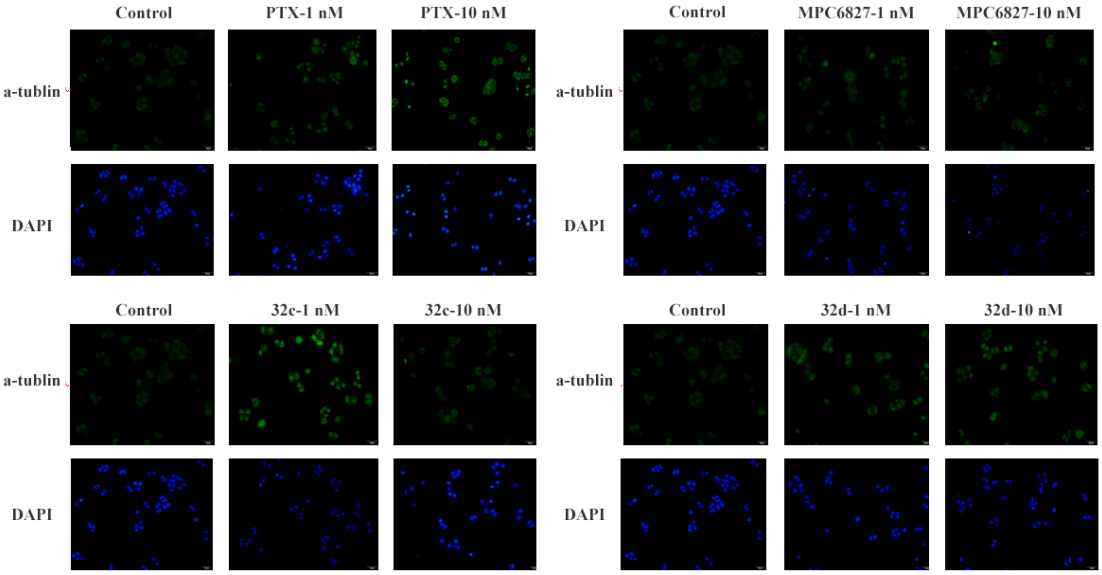

This article is protected by copyright. All rights reserved.

Accepted Article

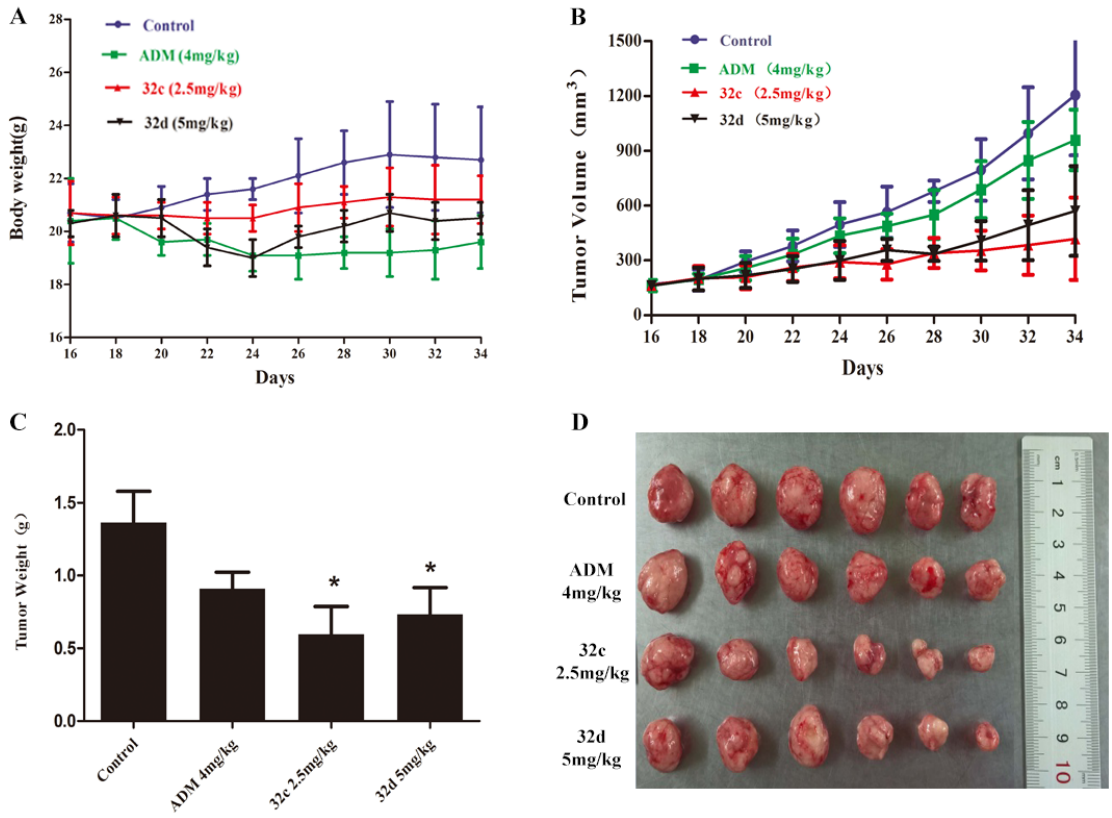

This article is protected by copyright. All rights reserved.

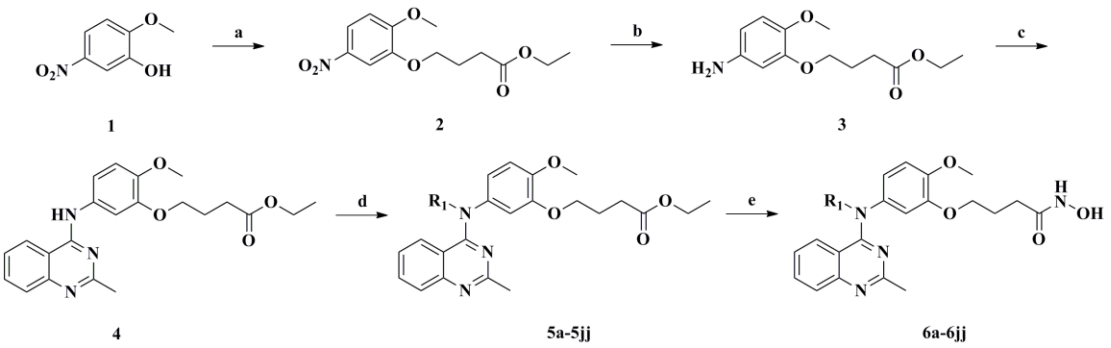

6a R_1= CH_2CH_3
6b R_1= $CH_2CH_2CH_2CH_3$
6c R_1= $CH_2CH(CH_3)_2$
6d R_1= $CH_2CH_2CH_2CH_2CH_3$
6e R_1= $CH_2CH_2CH_3$
6f R_1= $CH_2CH_2CH_2CH_2CH_2CH_3$
6g R_1= $CH_2C_6H_5$
6h R_1= m-$CH_2C_6H_4F$
6i R_1= o-$CH_2C_6H_4F$
6j R_1= CH_2CHCH_2
6k R_1= $CH_2CHC(CH_3)_2$
6l R_1= m-$CH_2C_6H_4OCH_3$
6m R_1= m-$CH_2C_6H_4CH_3$
6n R_1= 2',3'-$CH_2C_6H_3(OCH_3)_2$
6o R_1= m-$CH_2C_6HC_4OC_6H_5$
6p R_1= p-$CH_2C_6H_4OCH_3$
6q R_1= CH_2OCH_3
6r R_1= m-$CH_2C_6H_4OCHF_2$
6s R_1= 3',5'-$CH_2C_6H_3(CF_3)_2$
6t R_1= 2',5-$CH_2C_6H_3F_2$
6u R_1= 3'-F,4'-$CH_2C_6H_3NO_2$
6v R_1= $CH_2OCH_2CH_3$
6w R_1= $CH_2CH_2OCH_2CH_3$
6x R_1= $CH_2CH_2CHCH_2$
6y R_1= 3',4'-$CH_2C_6H_3F_2$
6z R_1= $CH_2CH_2C_6H_{11}$
6aa R_1= 2',4'-$CH_2C_6H_3F_2$
6bb R_1= 2',6'-$CH_2C_6HC_3F_2$
6cc R_1= p-$CH_2C_6H_4CF_3$
6dd R_1= p-$CH_2C_6H_4NO_2$
6ee R_1= p-$CH_2C_6H_4CH_3$
6ff R_1= o-$CH_2C_6H_4CH_3$
6gg R_1= 2'-F,4-$CH_2C_6H_3Cl$
6hh R_1= m-$CH_2C_6H_4C_6H_5$
6ii R_1= o-$CH_2C_6H_4NO_2$
6jj R_1= $CH(C_6H_5)_2$

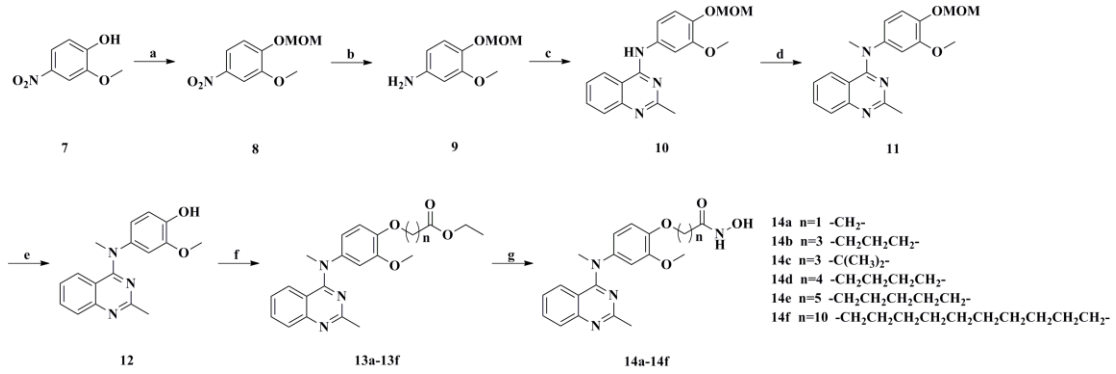

14a n=1 -CH_2-
14b n=3 -$CH_2CH_2CH_2$-
14c n=3 -$C(CH_3)_2$-
14d n=4 -$CH_2CH_2CH_2CH_2$-
14e n=5 -$CH_2CH_2CH_2CH_2CH_2$-
14f n=10 -$CH_2CH_2CH_2CH_2CH_2CH_2CH_2CH_2CH_2CH_2$-

This article is protected by copyright. All rights reserved.

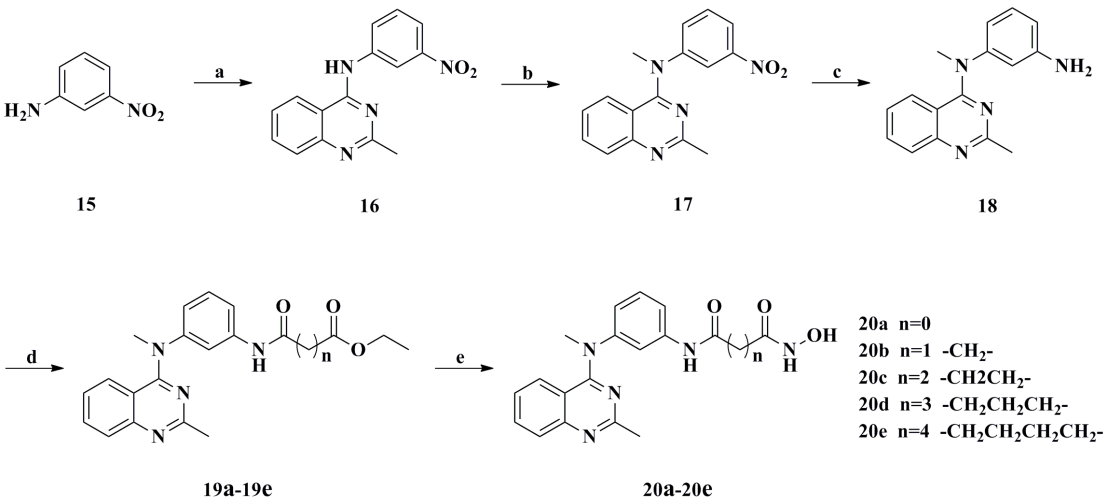

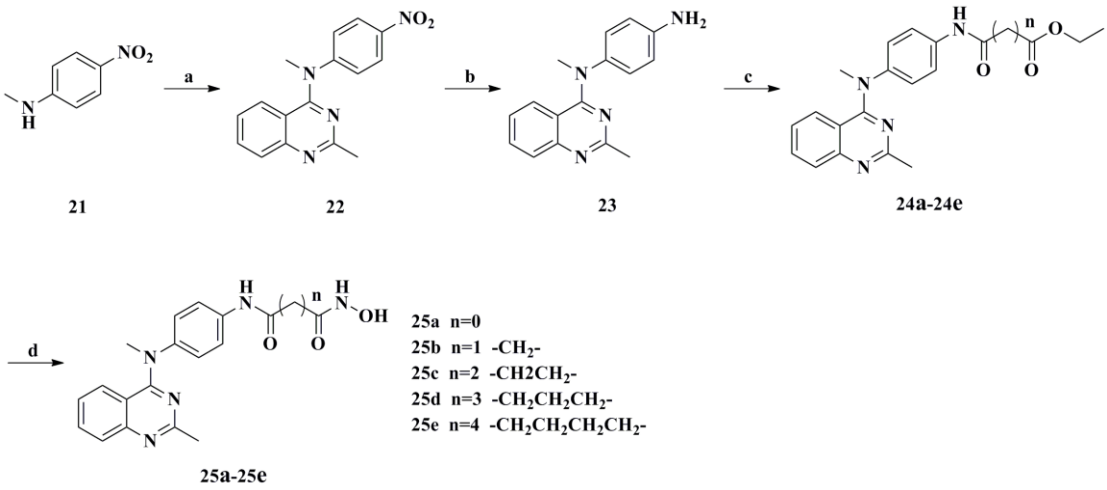

Accepted Article

This article is protected by copyright. All rights reserved.

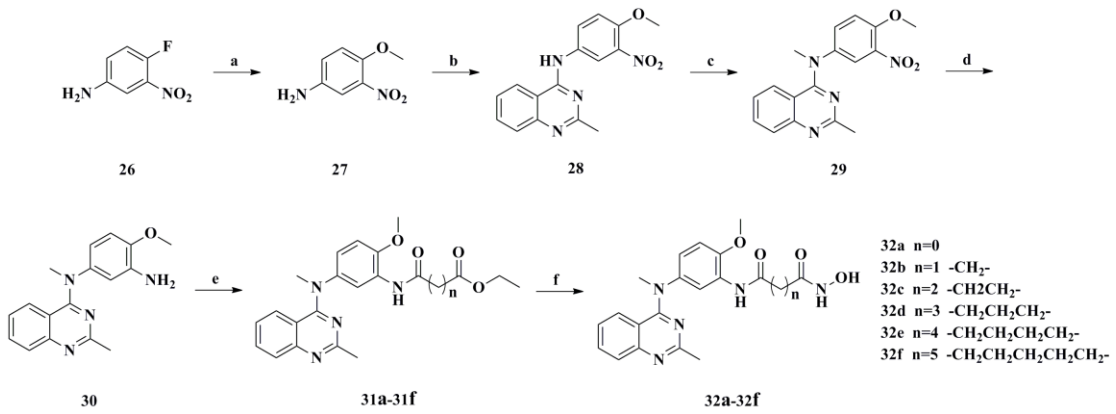

Accepted Article

This article is protected by copyright. All rights reserved.